SAND2021-15581C

Validation of Actuator Line and Actuator Disk Models with Filtered Lifting Line Corrections Implemented in Nalu-Wind Large Eddy Simulations of the Atmospheric Boundary Layer

Myra Blaylock[1], Brent Houchens[1], Lawrence Cheung[1]
Sandia National Laboratories, Livermore, CA, 94550, USA

Philip Sakievich[2], Alan Hsieh[3], Tommy Herges[4], and David C. Maniaci[5]
Sandia National Laboratories, Albuquerque, NM, 87185, USA

Luis A. Martinez-Tossas[6]
National Renewable Energy Laboratory, Golden, CO 80401-3305, USA

Turbine generator power from simulations using Actuator Line Models and Actuator Disk Models with a Filtered Lifting Line Correction are compared to field data of a V27 turbine. Preliminary results of the wake characteristics are also presented. Turbine quantities of interest from traditional ALM and ADM with the Gaussian kernel (ϵ) set at the optimum value for matching power production and that resolve the kernel at all mesh sizes are also presented. The atmospheric boundary layer is simulated using Nalu-Wind, a Large Eddy Simulation code which is part of the ExaWind code suite. The effect of mesh resolution on quantities of interest is also examined.

I. Nomenclature

a	=	characteristic velocity
ABL	=	atmospheric boundary layer
ADM	=	actuator disk model
ALM	=	actuator line model
c	=	blade chord length
CFD	=	computational fluid dynamics
D	=	diameter of the rotor
Δt	=	simulation time step
Δx	=	mesh size nearest the turbine
ϵ	=	smoothing length scale for the Gaussian kernel
LES	=	large eddy simulation
N	=	number of force points used in ADM and ALM
QoI	=	quantity of interest
SWiFT	=	Scaled Wind Farm Technology

II. Introduction

Computational fluid dynamics (CFD) is a common tool used to model the wind resource for wind plant operations and capture the quantities of interest (QoI) such as power production and loads on the turbines. The CFD provides a

[1] Principal Member of the Technical Staff, Thermal/Fluid Science & Engineering, AIAA Member.
[2] Senior Member of the Technical Staff, Computational Thermal & Fluid Mechanics
[3] Senior Member of the Technical Staff, Wind Energy Technologies Department.
[4] Senior Member of the Technical Staff, Wind Energy Technologies Department.
[5] Principal Member of the Technical Staff, Wind Energy Technologies Department, AIAA Member.
[6] Research Engineer, National Wind Technology Center

model of the atmospheric boundary layer (ABL) for neutral conditions and the turbines are represented by either the actuator line model (ALM) [1] or the actuator disk model (ADM). An important parameter for both of these models is the smoothing length scale for the Gaussian kernel ϵ [1], which is used to transfer the aerodynamic forces to the CFD cells as a body force, but choosing the correct value can be complex. ϵ needs to be large enough for the Gaussian kernel to be resolved by the fluid mesh. Previous literature has shown ϵ has a very significant influence on aerodynamic power [2], and in order to match the power production accurately, ϵ should be less than 0.035 D, where D is the rotor diameter [3,4]. This would allow for slightly larger ϵ values. However, for optimum blade loading, ϵ should be less that around 0.25 c, or a quarter of the chord length [5]. This would mean that ϵ would have to be quite small or change along the blade. The restrictions for optimum blade loads and power calls for a relatively fine mesh resolution in the area of the rotor blades, which can be computationally expensive. The application of a Filtered Lifting Line Correction (FLLC) [6] to the ALM and ADM corrects for both a non-optimal epsilon value as well as adding in the effects of the induced velocity that cannot be resolved from the mesh.

III. Objectives

In this study we will validate the power calculated with the FLLC by comparing to field data from Sandia National Laboratories' Scaled Wind Farm Technology (SWiFT) facility [7]. We will also look at any effects that the FLLC have on the wake generation. We will compare the quantities of interest (QoI) with traditional ALM and ADM calculations at varying grid resolutions. These will be run using an ϵ/D value of 0.035 to match the power production while balancing computational demands as recommended in previous work [3,4] as well as a larger ϵ/D that capture other grid scaling concerns. The minimum ϵ for the FLLC cases are based on the mesh spacing. A timing study will also help show that the FLLC is an excellent option to have more accurate power estimates without adding significant computational costs.

IV. Methodology

The OpenFAST software suite [9] developed at the National Renewable Energy Laboratory (NREL) is used to simulate the wind turbine dynamics. OpenFAST enables the analysis of complex physical and environment coupling, including turbine controllers, elastic dynamics, and flow-structure interactions with actuator line theory or actuator disk theory. The OpenFAST model of the Vestas V27 is used in the analyses to match the rotors used at the SWiFT facility [7, 10] during the experimental campaign. Meteorological and turbine data were taken during the wake steering experimental campaign at the SWiFT facility from 2016 to 2018, and the open-source data is available at the Atmosphere to Electrons' Data Archive Portal [11] and will be used to compare the results of this study.

To simulate the turbulent atmospheric boundary layer, the multiphysics, massively parallel large eddy simulation (LES) code Nalu-Wind, part of the ExaWind code suite, is used [12]. Nalu-Wind solves the Navier-Stokes equations in the low-Mach number approximation. A one-equation, constant coefficient, turbulent kinetic energy model for the subgrid scale stresses is used [2]. The simulation domain was taken to be 3km x 3km x 1km in the x, y, and z directions, and one wind turbine is placed in the center of the domain for a neutral ABL case. The meshes and selection of the ten-minute period of time used to compare to the field data is described in Hsieh *et al*. [13]. Throughout this paper, Δx refers to the portion of the mesh nearest the turbine, which is always the most resolved region in the domain.

Following [1], the fluid-structure interaction that the turbine imposes on the wind is simulated by adding a body force f_i in the momentum equation. The standard equations for actuator models are of the form

$$f_i = \int_0^L F_i(l)\, g(\vec{r})\, dl \tag{1}$$

where l is the distance along an actuator line and Fi are actuator line forces computed from the incoming velocity flow and the airfoil characteristics specified in OpenFAST. The smoothing kernel $g(r)$ has the form

$$g(r) = \frac{1}{\epsilon \pi^{3/2}} exp\left(-\frac{r^2}{\epsilon^2}\right) \tag{2}$$

where ϵ is a characteristic length scale that determines the volume over which the body forces are spread. For the ADM, the same smoothing functions are used, but the kernel points are placed azimuthally between the actuator line points with the same spacing as is applied along the actuator line blades. Figure 1 shows the force distribution for ALM and ADM. These cases have enough points along the blade that the smoothing kernels overlap, so the multiple points appear to be lines.

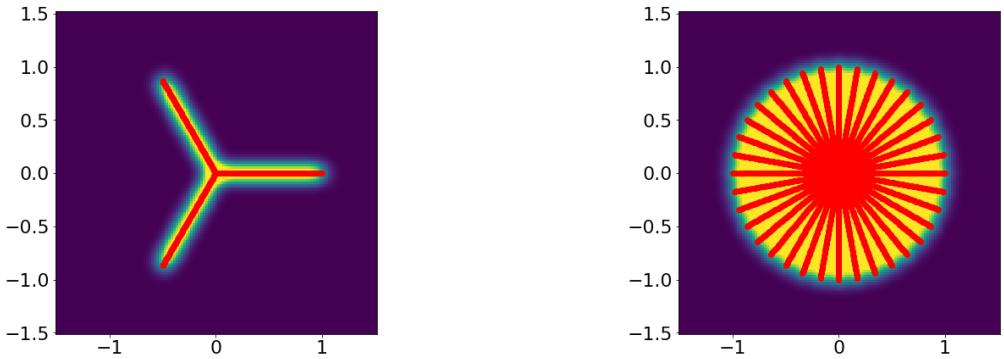

Figure 1. Visualization of ALM (left) and ADM (right). The axes are scaled by the rotor diameter. The coloring shows the Gaussian distribution of the forces. The lines of the ALM, representing the blades, will turn, while the ADM points are stationary.

The application of the FLLC is described in detail in Martínez-Tossas and Meneveau [6]. Like the traditional ALM model, it first computes the forces from the aerodynamic model of the blade. It then calculates the gradient of the lift distribution along the blade. The induced velocity from the gradient of the lift is found using both a specified ϵ and also an $\epsilon_{\text{optimum}}$. The latter is the value expected to produce the optimum simulation accuracy for blade loading, which previous research has related to the chord of the blade c as $\epsilon_{\text{optimum}} = 0.25c$ [8]. Typically, this optimum value is too small to be practical for simulations, and results in errors like the Runge phenomenon appearing in the simulation if the grid is not scaled accordingly [5]. For example, the chord of a V27 varies from 1.3 m near the root to 0.5 m near the tip. This results in an $\epsilon_{\text{optimum}}$ of less than 0.325 m. However, to also comply with the recommendation that $\epsilon/\Delta x \geq 5$ from [5] would then require Δx be less than 0.065 m. This is approximately five times smaller than the finest mesh used in this study and would yield practically untenable computational times.

In both this work and a previous study [6], the optimum value for the FLLC has been taken as $\epsilon_{\text{optimum}} = 0.25c$ along the blade. A velocity correction term is set to be the difference between these two induced velocities. The forces for the actuator line are then computed using the velocities plus this correction term. In this study the minimum ϵ was set to be twice the size of the grid resolution nearest the turbine.

Results based on ALM and ADM are compared for two values of ϵ and four mesh resolutions as illustrated in Figure 1 and Table 1. These combinations produce the range of $\epsilon/\Delta x$ values given in Table 1. The goal of this work is to determine which $\epsilon/\Delta x$ values or range of values are most appropriate for each model and to compare the FLLC to the traditional ALM and ADM. The authors also note that, to the best of their knowledge, this is the first time that the FLLC has been applied to ADM in published literature. In order to apply the FLLC to ADM the same aerodynamic model is used for both ALM and ADM. In these models the same OpenFAST turbine model is used to generate the aerodynamic forces, and the only difference between ALM and ADM is the spreading methodology. For the ADM the aerodynamic force at a given radial location is averaged and then spread uniformly in the azimuthal direction via multiple actuator points, while the ALM just applies the computed forces locally with a single Gaussian kernel for each force point computation from the aerodynamic model.

$\epsilon/D = 0.1$ is an upper limit of for what is appropriate [2,3] but resolves the epsilon for mesh sizes in this study, and $\epsilon/D = 0.035$ should be an optimum ratio for blade loading [3,4]. For the Vestas V27 rotor, these yield $\epsilon = 2.7$ m and $\epsilon = 0.945$ m, respectively. Table 1 shows the mesh sizes used and the resulting $\epsilon/\Delta x$ values.

Table 1. $\epsilon/\Delta x$ for the various meshes, based on refinement Δx near the turbine and ϵ/D values investigated.

	Extra Coarse Δx = 2.5 m	**Coarse** Δx = 1.25 m	**Medium** Δx = 0.625 m	**Fine** Δx = 0.3125 m
$\epsilon/D = 0.1$ (ϵ = 2.7 m)	1.08	2.16	4.32	8.64
$\epsilon/D = 0.035$ (ϵ = 0.945 m)	0.378	0.756	1.512	3.024
FLLC (min $\epsilon = 2*\Delta x$)	2	2	2	2

A timing study was also completed to compare the traditional ALM, ADM, and FLLC methods. As shown in the results, the FLLC adds a small amount of computational time, but we are expecting that it will be on the order or smaller than the effect of changing the number of points used for the calculation or changing ϵ in a traditional method.

Switching from ALM to ADM affects the time step that can be used. The maximum time step determined by the Courant–Friedrichs–Lewy number (CFL) for each model is based on different velocities in the problem.

$$\mathrm{CFL} = a\frac{\Delta t}{\Delta x} \tag{3}$$

where a is the characteristic velocity, Δt is the maximum time step and Δx is the mesh size nearest the turbine. Time steps were selected to maintain a CFL of near the ideal value of one for convergence.

The characteristic velocity for the ALM is the tip speed of the blade. For the V27 turbine, the blades are 13.5 m long and the rotational speed in this simulation is set to 42 rpm. This leads to a tip velocity of 59 m/s and a maximum $\Delta t = \Delta x/59$ s for CFL = 1. However, the characteristic velocity for the ADM is the wind speed since there are no moving blades in the model. Therefore, with a wind velocity of 8.3 m/s, the maximum $\Delta t = \Delta x/8.3$ s. This difference in characteristic velocity significantly reduces the total number of time steps, and thus the computational cost, needed for the ADM compared to the ALM to simulate a given time duration. This ADM efficiency becomes more pronounced for turbines with larger tip speeds compared to the wind velocity. Conversely, the ADM method requires evaluation at more actuator points at each time step, somewhat offsetting the gains in increased time-step size. For the ALM cases, we used a time step which resulted in the tip of the blade traveling a distance of two grid spaces. The resulting time step values used in the simulations are given in Table 2. The time steps for the FLLC cases are the same as the corresponding ADM and ALM cases for each mesh.

Table 2. Maximum time step for each mesh and turbine model.

	Extra Coarse Δx = 2.5 m	**Coarse** Δx = 1.25 m	**Medium** Δx = 0.625 m	**Fine** Δx = 0.3125 m
Δt for ALM ≈ $2\Delta x/59$ [s]	0.08	0.04	0.02	0.01
Δt for ADM ≈ $\Delta x/8.3$ [s]	0.29	0.14	0.07	0.03

V. Results

We compare both the turbine QoI's and wake QoI's to the field data recorded at the Scaled Wind Farm Technology (SWiFT) site [7]. A detailed study found a section of the data with a10 minute average of Generator Power from the experimental field of 79.1+/- 20.1 kW [13], and we compare the generator power for this 10 minute period as well as showing time integrated forces along the blade. Preliminary results from wake data is also shown.

A. Grid Resolution Study -ALM & ADM

To establish a baseline of which values can be expected and what grid resolution is adequate for the traditional (non-FLLC) models, we will compare the simulations for ALM and ADM at the four grid resolutions described in Section IV. Based on the work by *Hsieh, et al.* [13], theses simulations match a period of time with a velocity 10 minute average from the SWiFT site with a neutral boundary layer of a value for generator power of 79.1 ± 20.1 m/s. This mean value is shown in all the generator power figures as a dashed line, and the standard deviation as a light blue region.

A qualitive example of the wake at 0.5 D downstream of the turbine for the ALM, $\epsilon/D = 0.035$, case is shown in Figure 1. Previous work [4, 14] has shown that $\epsilon/D = 0.035$ gives a more accurate result for the generator power than $\epsilon/D = 0.1$ for ALM, so only that value is shown in Figure 2.

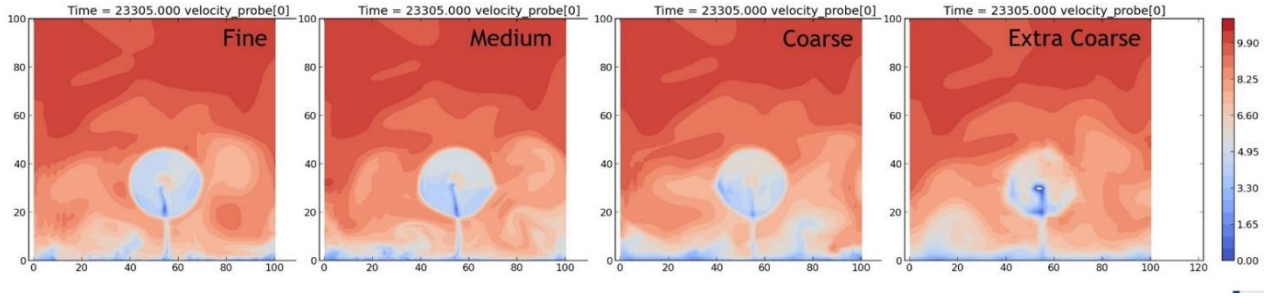

Figure 2. Four mesh resolutions at 0.5 D downstream. The simulation used the ALM with $\epsilon/D = 0.035$.

The generator power plot in Figure 2 shows that the medium and fine meshes match the observed generator power from the SWiFT site better than the coarse and extra coarse meshes. The normal and tangential forces and the axial velocity along the blade, averaged over the 10 min period from 60 to 660 s, also shows that the two finer meshes are in closer agreement than the two coarser grids. This is due to the ϵ/D value being too small for those two mesh sizes. We will go into more detail in the discussion of the ADM grid resolution.

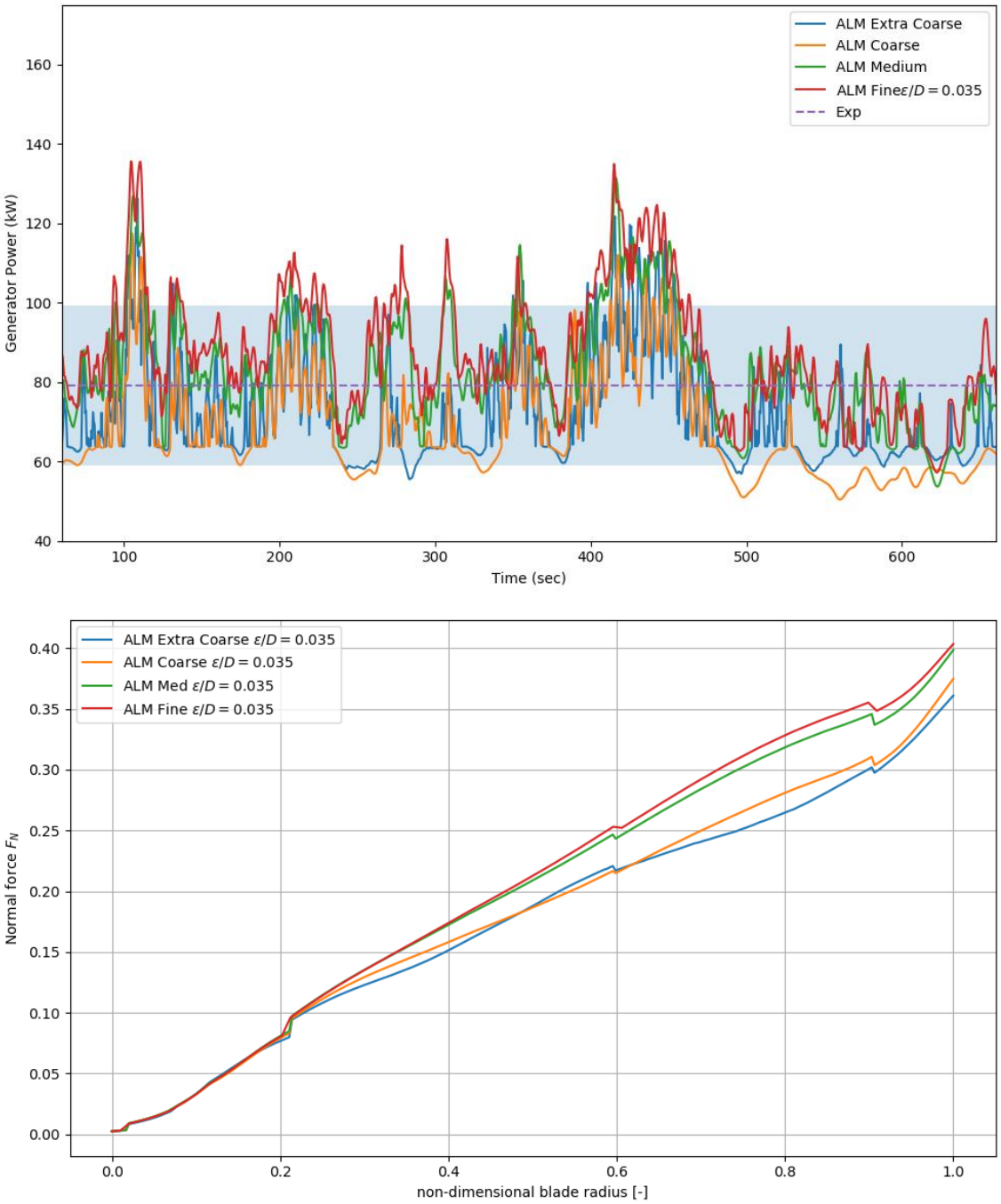

Figure 3. Grid resolution study showing generator power predicted and the normal force for ALM for $\epsilon/D = 0.035$. Average experimental values are also shown for power.

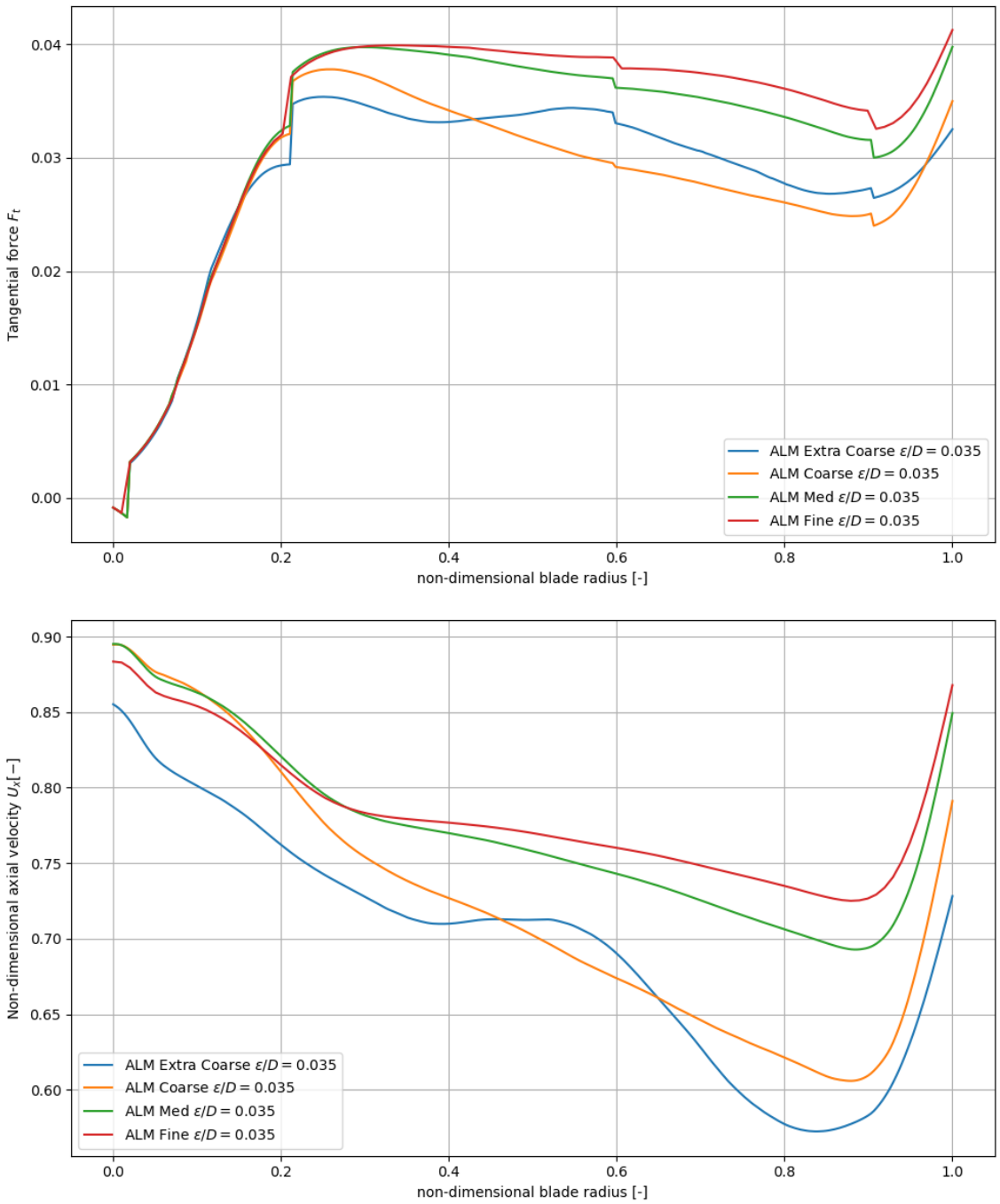

Figure 4. Grid resolution study showing the tangential force and axial velocity for ALM for $\epsilon/D = 0.035$.

For a reference for what is the "most correct" simulation, fine mesh values for generator power based on the ALM with small ϵ are shown as open circles in subsequent plots. To show that the same ϵ/D trends also hold for the ADM, simulations for both ϵ/D values are plotted side by side in Figure 5. The time series of the generator power is shown as well as profiles along the blade for the non-dimensional normal forces, tangential forces, and axial velocities. Experimental data for the generator power mean (dashed line) and standard deviation (light blue region) is also provided as a reference. The ALM and ADM with both ϵ/D values are shown together in the next sub-section.

ADM, $\epsilon/D = 0.035$ ADM, $\epsilon/D = 0.1$

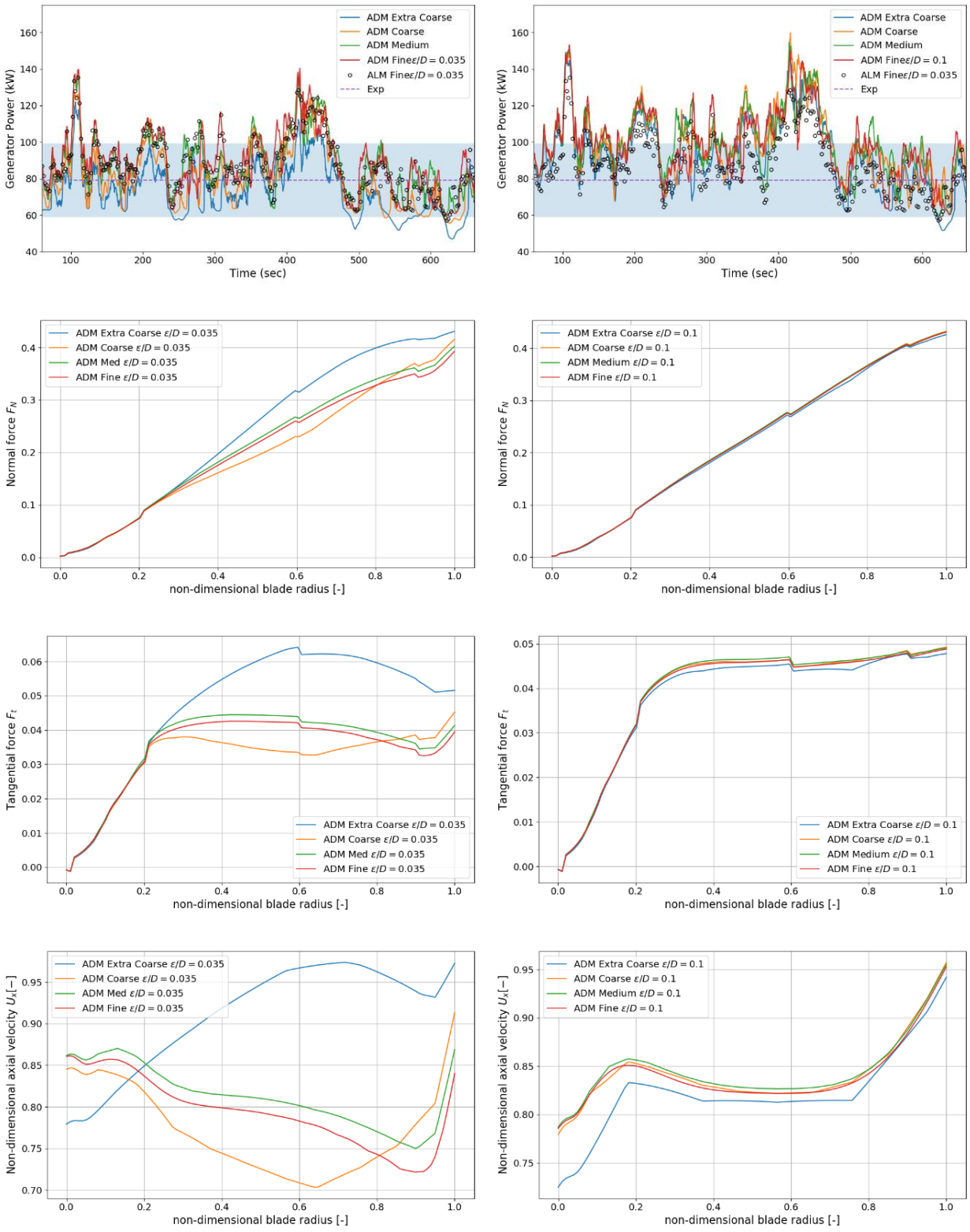

Figure 5. Grid resolution study for ADM at two ϵ/D values.

Several trends are observed in the plots above. For corresponding meshes, the larger ϵ simulations produced significantly larger generator power predictions than the smaller ϵ results. The blade profiles for the larger ϵ simulations are very similar and do not show much deviation with mesh resolution. On the other hand, the blade profiles for the smaller ϵ cases differ significantly by mesh level, especially for the ADM Extra Coarse results, indicating that this mesh is not converged with the larger mesh spacing. The larger ϵ produces more robust, converged results, but over-predicts power as the rotor is effectively spread over a larger area than what is physical, so it is recommended to use a smaller ϵ , despite needing a finer mesh.

These trends can be attributed to the incorporation of the ϵ term within the traditional ADM model. For the larger ϵ results, the radial distribution of the actuator forces is much larger than the mesh resolution even for the ADM Coarse case, resulting in little changes of results with mesh resolution. However, this large ϵ value is much larger than recommended and is considered less accurate than those using a smaller ϵ value. For the smaller ϵ results, where the minimum mesh resolution is on the same order as ϵ, the ADM Coarse and Medium profiles show that the mesh resolution for those cases is not large enough to adequately resolve the spreading of the actuator forces. The blade profiles for these cases are significantly different than those observed in the larger ϵ cases. ~~Only the ADM Fine case using the smaller ϵ is able to produce blade force and velocity profiles similar to the larger ϵ cases and is considered the most accurate of the presented simulations with ϵ being much closer to its optimal value~~[BML1].

B. ADM &ALM ϵ/D Dependence

Figure 6 to Figure 9 show comparisons of the generator power, forces, and velocities at a single mesh resolution (medium) between the traditional ADM and ALM models. The effect of ϵ for both ADM and ALM is pronounced, with the higher epsilon cases producing significantly larger power, force, and velocity predictions than the lower epsilon cases. The differences along the blade profiles due to ϵ are especially pronounced near the blade tips. The ADM model is shown to produce larger predictions of power, force, and velocity compared to the ALM model. This shows the impact of the strong impact of the disk geometry on these quantities of interest since the ALM and ADM are both using the same aerodynamic model in this study. The smaller ϵ cases produced generator power predictions closer to the experimental power reference, demonstrating that the smaller ϵ used is indeed closer to optimal and produces results that are more accurate than the larger ϵ.

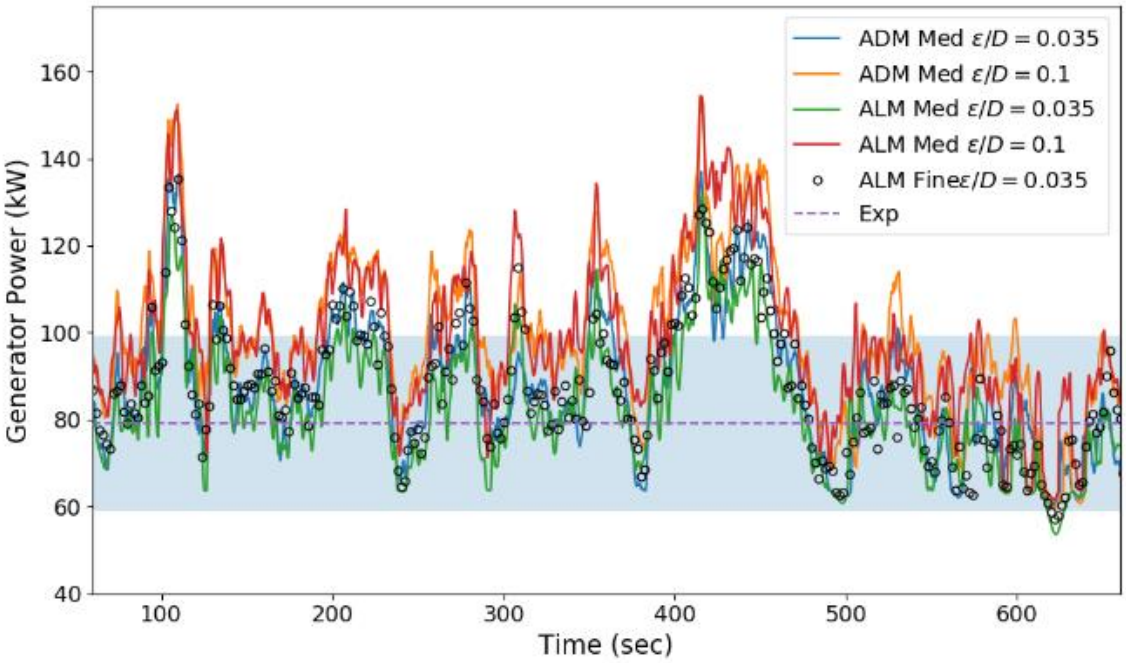

Figure 6. Generator power for both ϵ/D values from the medium mesh ADM and ALM simulations and comparison to ALM fine and experimental data.

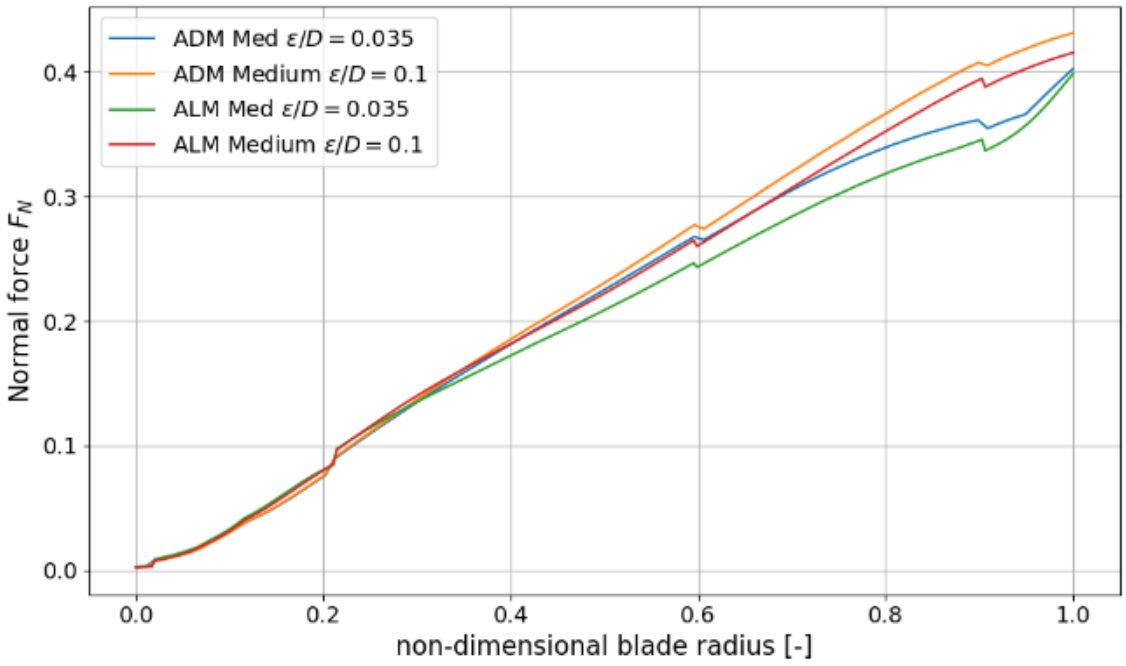

Figure 7. Normal force for both ϵ/D values from the medium mesh ADM and ALM simulations.

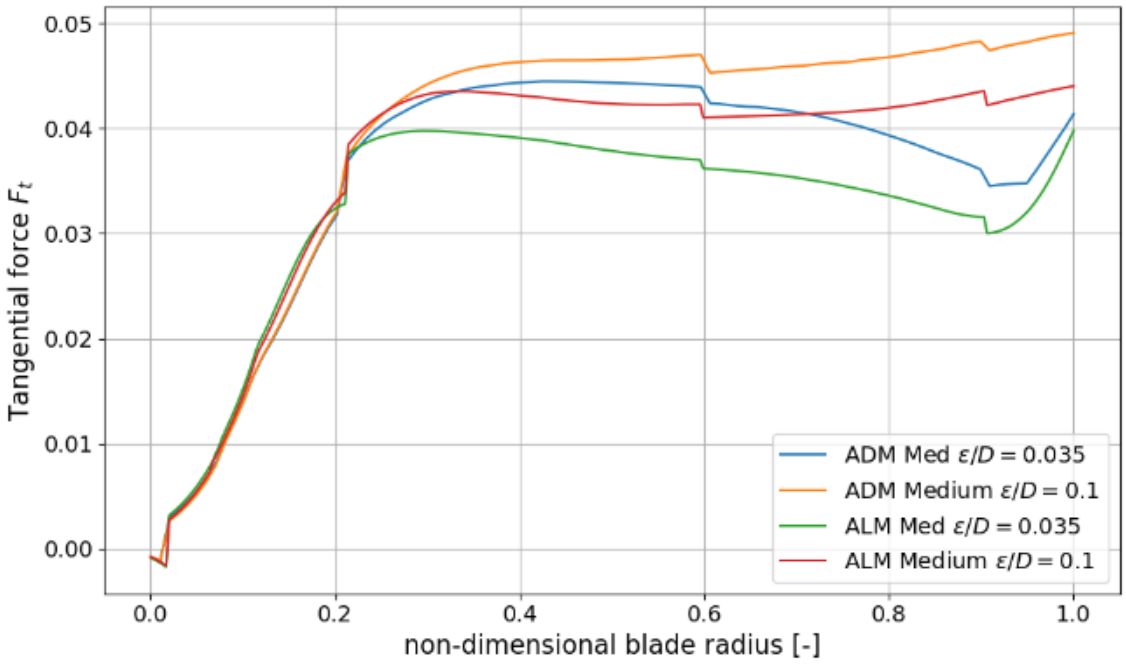

Figure 8. Tangential force for both ϵ/D values from the medium mesh ADM and ALM simulations.

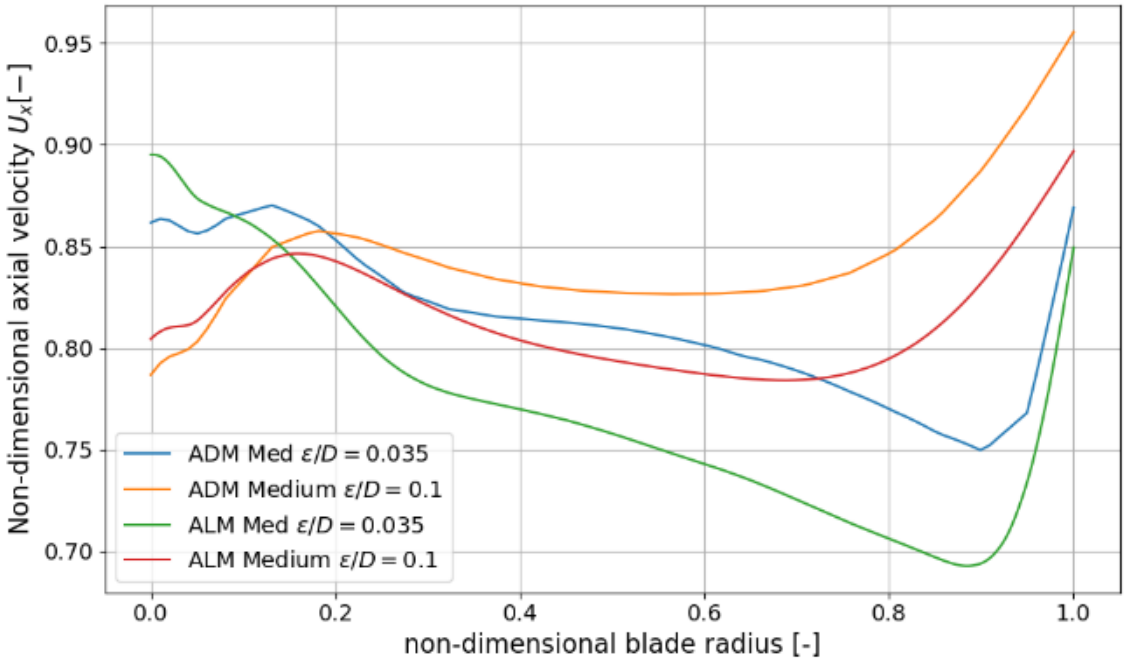

Figure 9. Axial velocity for both ϵ/D values from the medium mesh ADM and ALM simulations.

C. Grid Resolution Study - Filtered Lifting Line Correction

Figure 10 shows the FLLC-ALM and FLLC-ADM models for times series of generator power, along with non-dimensional normal force, tangential force, and axial velocity profiles along the blade. In contrast to the traditional ADM results shown previously, the FLLC profiles show little sensitivity to mesh resolution and are able to capture the aerodynamic phenomena occurring at the blade tips. The FLLC method prevents the Runge phenomena for the coarse and extra coarse mesh, allowing for more physically meaningful solutions for these efficient meshes while still allowing for use of the more computationally affordable meshes. In short, the FLLC model is able to avoid the issues observed in both the higher and lower epsilon cases using the traditional actuator models. It corrects for the offset observed in the higher epsilon cases and overcomes the inability of the mesh resolution to resolve the previous epsilon term in the lower epsilon cases.

Visualizing the flow field can give insight to why the FLLC method yields a more grid resolved solution. As mentioned before, when the ϵ/D value is too small for a given grid resolution, there is a resulting effect that can cause the Runge phenomenon to appear in front of the turbine [5]. This can be seen in the left column of Figure 11, which shows the extra coarse, coarse, medium, and fine meshes from top to bottom, respectively. These lines are apparent in the extra coarse and coarse grid, but have disappeared in the medium and fine grids. The force correction along the blade direction from the FLLC alleviates this issue, allowing for more physically meaningful solutions for these efficient meshes, as seen in the right hand column of the same figure.

FLLC-ADM FLLC-ALM

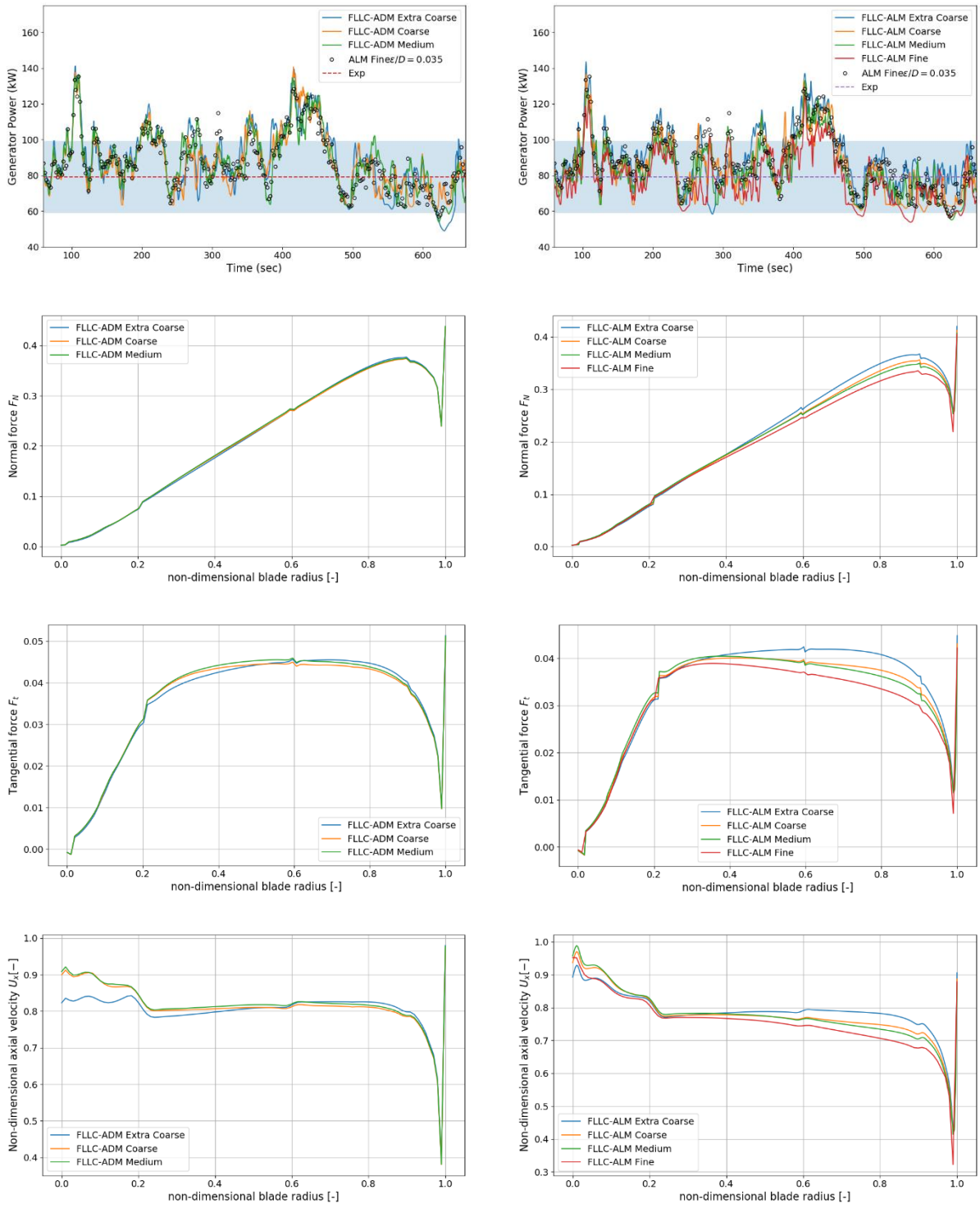

Figure 10. FLLC-ADM (left column) and FLLC-ALM (right column) grid resolution studies.

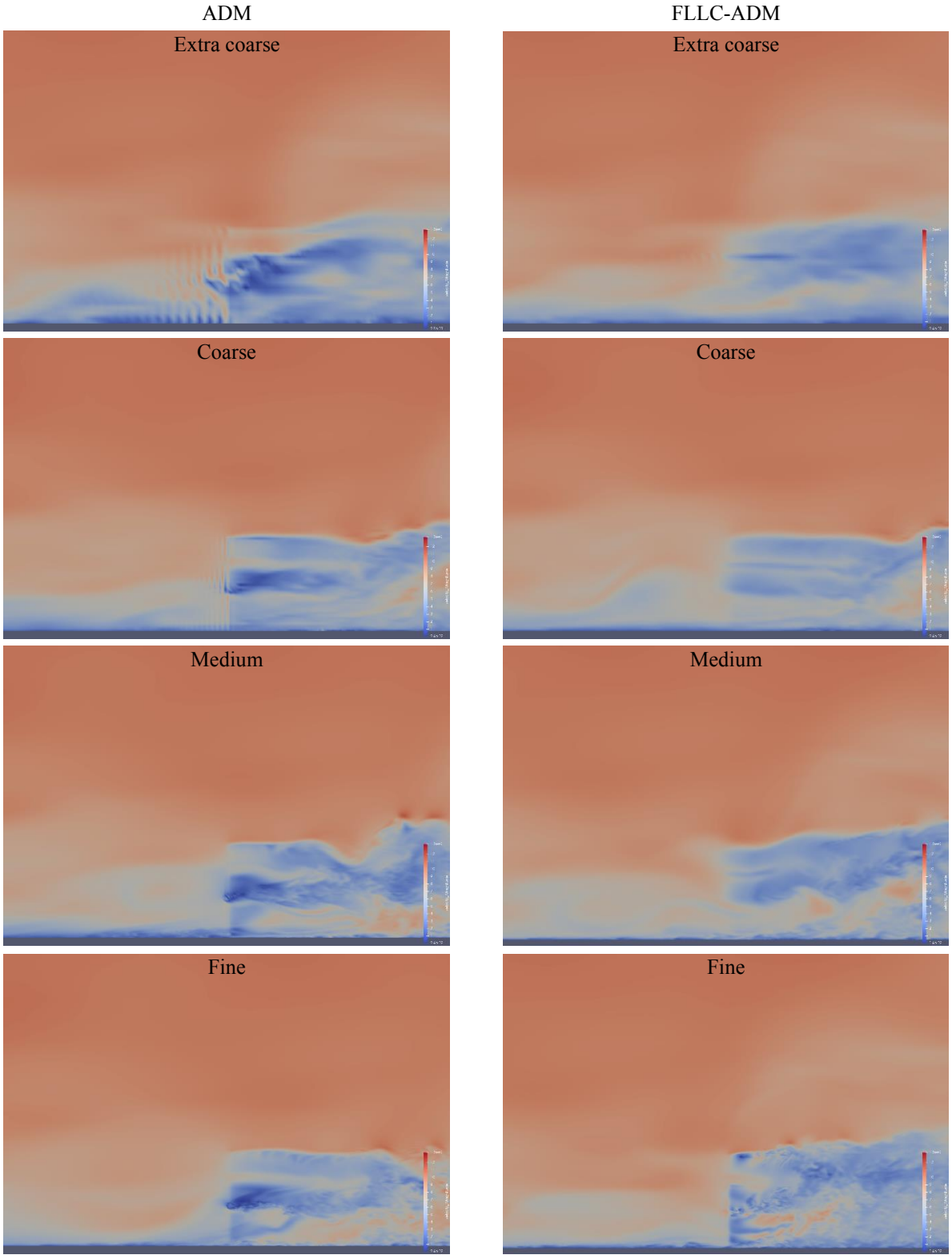

Figure 11. Cross-section of the velocity flow field at the midline of the turbine. Left column shows ADM without FLLC, right column shows FLLC-ADM. Rows from top to bottom are for the extra coarse, coarse, medium and fine meshes.

D. ADM – ALM – FLLC Comparison

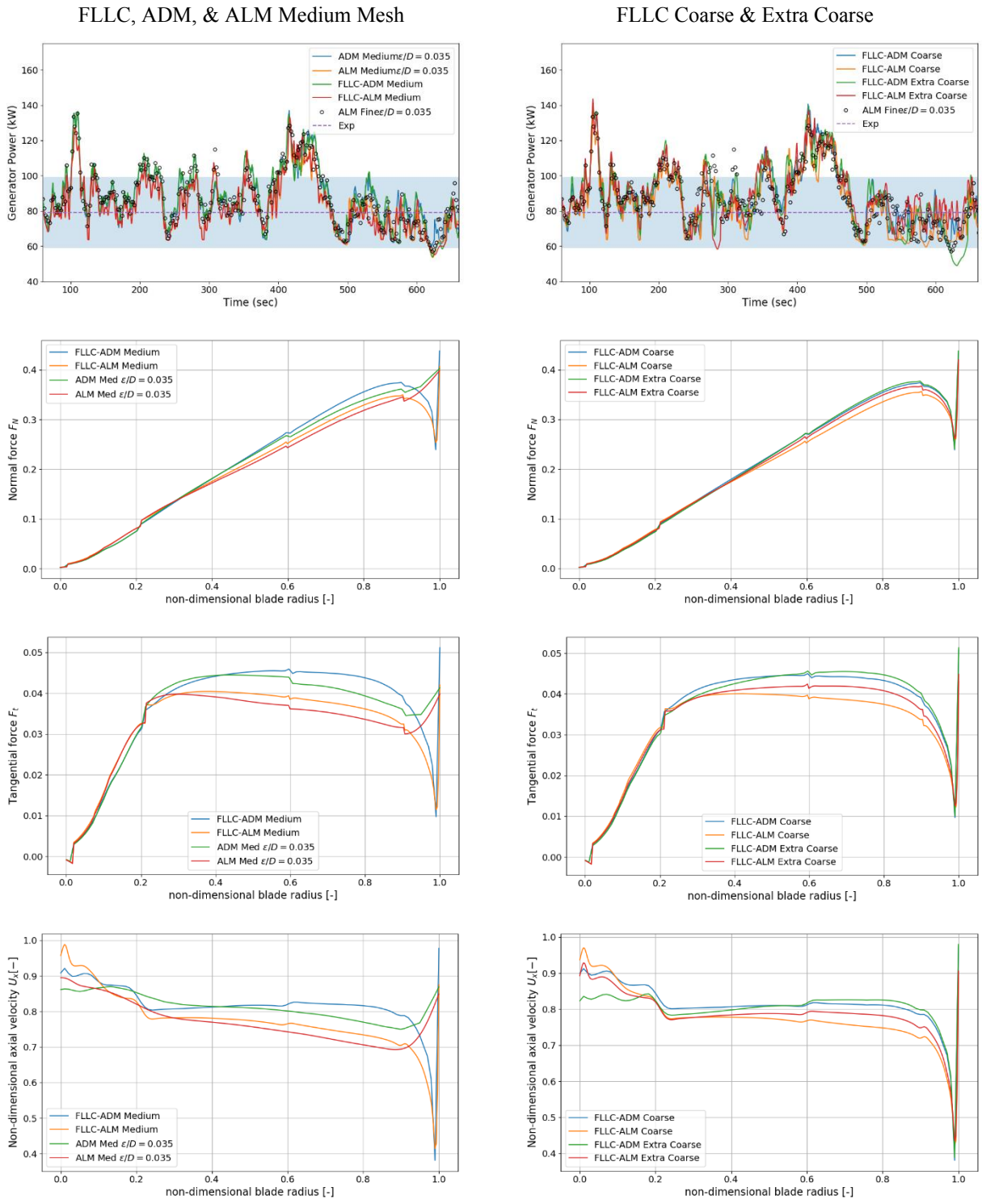

Figure 12. Comparison of the FLLC-ADM, FLLC-ALM, ADM and ALM for the medium mesh (left column). Comparison of the coarse and extra coarse meshes for the FLLC-ADM and FLLC-ALM (right column).

With the lower epsilon, fine mesh case demonstrated to be the most accurate for the traditional model, the above figures compare the traditional ALM and ADM results with the FLLC-ALM and FLLC-ADM results for power, forces, and velocity. For power, the FLLC results correspond very well with the traditional model results for both the ALM and ADM. But for the blade profiles of axial velocity and normal and tangential forces, the FLLC-ALM and FLLC-ADM results show more accurate approximation of these quantities, especially in the region near the blade tips. Figure 8 also shows that the velocity deficit at 0.5 D downstream of the turbine qualitatively matches in the FLLC-ALM case and the $\epsilon/D = 0.035$ case. In summary, the FLLC-ALM and FLLC-ADM models produce equivalent power predictions to the most accurate traditional ALM and ADM models, plus better approximations of the blade distributions of forces and velocities. This is especially noteworthy for the ADM since the geometric entity of the disk adds an additional source of error to the computation of these terms.

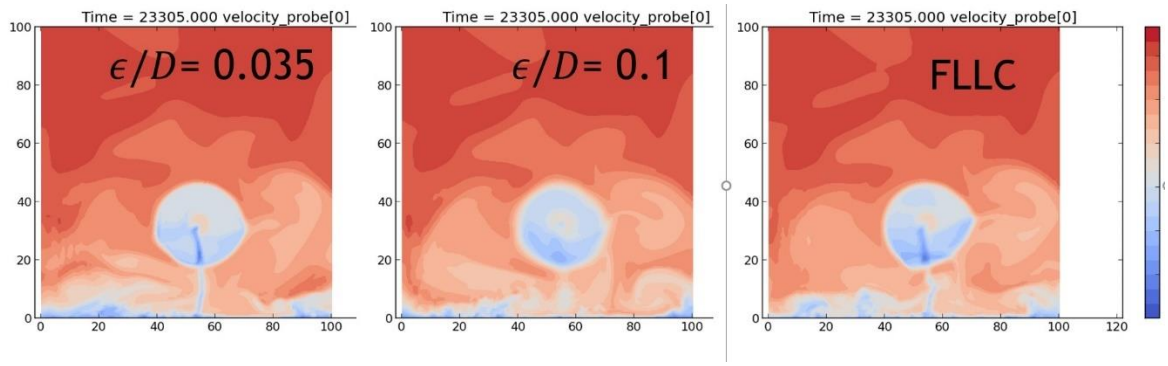

Figure 13. Velocity deficits showing the wake at 0.5 D downstream from traditional ALM and FLLC on the medium mesh [14].

E. Timing Comparisons

To compare simulation times for the ALM turbine models and at various mesh resolutions, several cases were run from the beginning of the simulation for 10 steps on 768 cores. Because the meshes need different time steps, the ten steps will produce different simulations times. Table 3 shows the time step for each mesh size, the CPU time needed for 10 steps, and the calculated wall time for that case to reach 1 minute of simulation time (assuming the first 10 steps scale linearly to one minute). Comparing the FLLC-ALM method to the non-FLLC case on the same mesh (medium), the FLLC-ALM is not slowed down by the FLLC implementation and was actually slightly faster for this scenario.

Since the FLLC method allows the user to have a coarser mesh with the same accuracy in power prediction, the overall duration of the simulation can be reduced by using a coarser mesh and the FLLC method. A similar study for the FLLC-ADM method will be done in future work.

Table 3. Timing for various turbine models and mesh refinements.

Turbine Model and Mesh Resolution	Δt (sec)	Wall Clock Time for ten steps (sec)	Calculated Wall Clock Time for 1 min of simulation time (sec)
ALM Med Mesh	0.02	141.771	42,531
FLLC-ALM Med Mesh	0.02	138.293	41,488
FLLC-ALM Coarse Mesh	0.04	140.722	21,108
FLLC-ALM Extra Coarse Mesh	0.08	126.816	9,511

F. Wake Comparisons

Here we will show a preliminary look at how the FLLC method affects the wakes of the turbine. Figure 14 shows the averaged normalized velocity field for the experimental data [15] as well as the ALM method and the FLLC-ALM method. For these time averaged quantities, the FLLC method qualitatively has very similar results compared to the non-FLLC method. A more thorough, quantitative study of this will presented in future work.

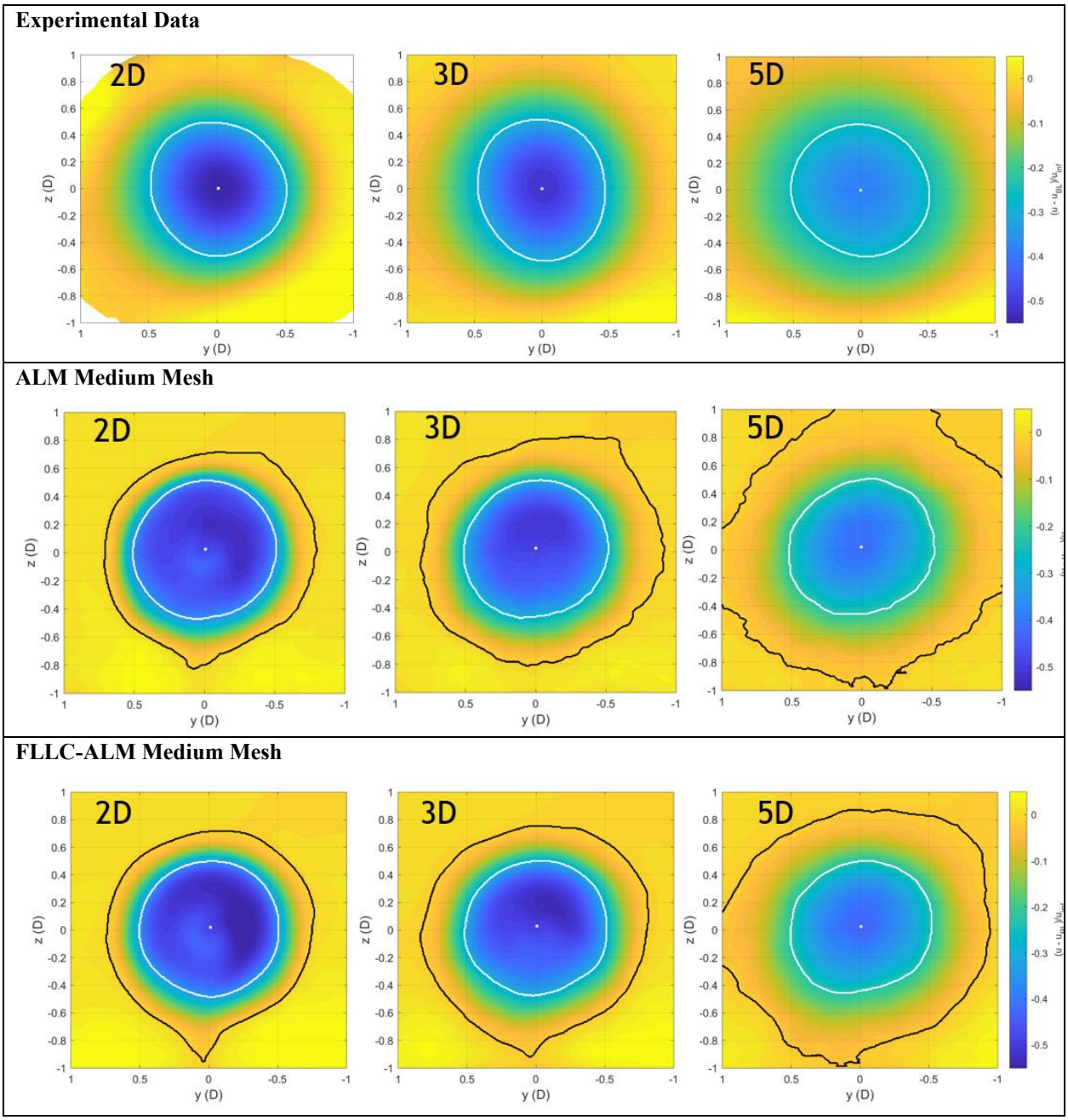

Figure 14. Experimental data of mean wake from lidar measurements (Top) is the same dataset that we used to compare to the Nalu-Wind simulations using the medium grid with ALM method and $\epsilon/D = 0.035$ (Middle) and the FLLC-ALM using the medium mesh (Bottom). Experimental wake data are planes in the meandering frame of reference (MFoR) for a neutral atmospheric benchmark, with dashed black lines marking the rotor

outline. Simulation data is also in the MFoR. The white line shows the wake defined with the same area as the rotor and the black line shows the wake defined using the converged thrust method.

Table 4 compares from the plane that is 2D downstream from the turbine an instantaneous snapshot of the velocity, the horizontal and vertical positions and standard deviations of the center of the wake, and the velocity deficit. The outline of the wake is defined by taking the velocity contours, starting with the minimum, where the deficit is the largest, and expanding the included contours for higher velocity values until the area defined by the highest value contour (shown as a white line) is the same as the rotor area. The center is found from a weighted centroid of velocity this area. To calculate the velocity deficit, the area of the wake is defined by where the thrust integrand converges towards zero at the edge of the wake in the meandering frame [13]. The velocity deficit is the maximum velocity minus the minimum velocity within that defined area of the 10 minute averaged MFoR wake. The center position is very constant for all cases. The velocity deficit is predicted to be larger for coarser meshes and for ADM compared to ALM.

Table 4. Wake comparisons for several cases.

Case	Wake plane at 2D downwind	Wake Position (m) Standard Deviation	Velocity Deficit (m/s)
ALM Fine Mesh	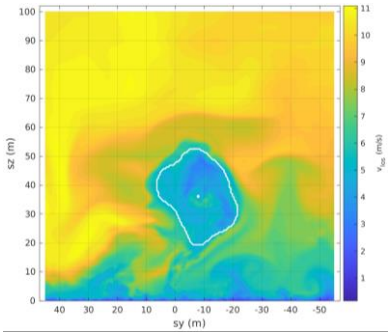	[1.5, 32.6] [4.8, 2.5]	-1.75
ALM Med Mesh	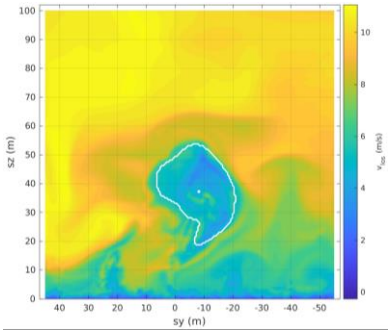	[-1.3, 33.0] [3.3, 1.9]	-1.57

ADM Med Mesh	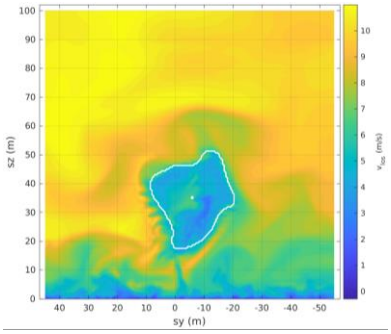	[-1.4, 33.0] [3.5, 2.1]	-1.67
FLLC-ALM Coarse Mesh	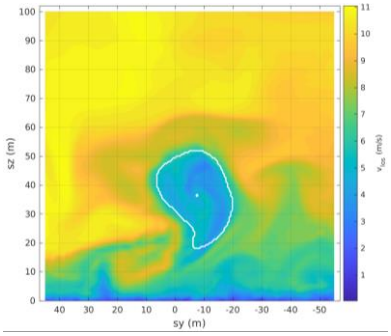	[-1.4, 33.1] [3.3, 2.0]	-1.93
FLLC-ADM Coarse Mesh	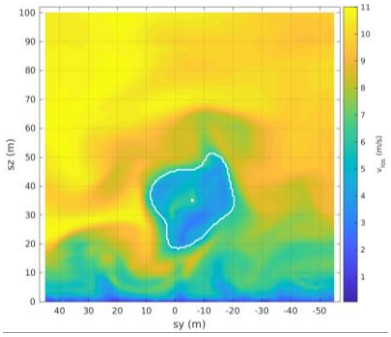	[-1.5, 33.0] [3.4, 2.0]	-2.01
FLLC-ALM Extra Coarse Mesh	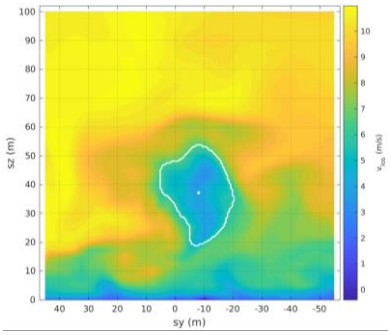	[-1.4, 33.0] [3.2, 2.0]	-2.42

FLLC-ADM Extra Coarse Mesh	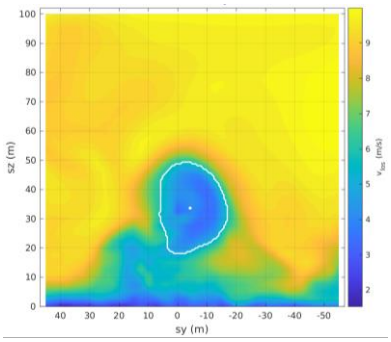	[-1.3, 32.9] [3.5, 2.0]	-2.43

VI. Conclusion

In this work, we performed large-eddy simulations of the atmospheric boundary layer at different grid resolutions with a turbine represented using actuator line and actuator disk models. The FLLC was used to correct the blade loading in the actuator disk and line models with the goal of achieving grid-independent solutions. The quantities along the blade were compared between the different simulations and power output was compared to experimental results. This is also the first time that the FLLC (developed originally for the actuator line model) has been tested in the actuator disk model.

The smaller ϵ cases produced generator power predictions closer to the experimental power reference, demonstrating that the smaller ϵ used is indeed closer to the optimal epsilon and produces results that are more accurate than the higher epsilon. This result is consistent with previous studies [3, 4, 5, 6, 8, 13].

The FLLC was able to reduce the difference in blade loading between simulations with different grid resolutions. It can also avoid the issues observed in both the higher and lower epsilon cases using the traditional actuator models. It corrects for the offset observed in the higher epsilon cases and overcomes the inability of the mesh resolution to resolve the previous epsilon term in the lower epsilon cases.

The FLLC method appears in Figure 11 to prevent the Runge phenomena for the coarse and extra coarse mesh, allowing for more physically meaningful solutions for these efficient meshes as indicated in the mean power results. The results presented with the FLLC used a minimum value of $\epsilon/\Delta x=2$. It seems that the results have not reached grid independence and future work should focus on extending the study with values of $\epsilon/\Delta x>2$ to find when convergence is reached.

A comparison of computational costs when using ALM, and FLLC-ALM shows that the FLLC-ALM method allows for faster simulations because a coarser grid can be used with similar results for generator power. Future work will confirm whether this outcome holds when also looking at wake distributions and will also explore FLLC-ADM.

In summary, the FLLC-ALM and FLLC-ADM models produce equivalent power predictions to the most accurate traditional ALM and ADM models, plus better approximations of the blade distributions of forces and velocities.

Acknowledgments

This research was supported by the Wind Energy Technologies Office of the US Department of Energy Office of Energy Efficiency and Renewable Energy. Sandia National Laboratories is a multimission laboratory managed and operated by National Technology & Engineering Solutions of Sandia, LLC, a wholly owned subsidiary of Honeywell International Inc., for the U.S. Department of Energy's National Nuclear Security Administration under contract DE-7 NA0003525. The views expressed in the article do not necessarily represent the views of the U.S. Department of Energy or the United States Government. SAND2020- XXXA

This work was authored in part by the National Renewable Energy Laboratory, operated by Alliance for Sustainable Energy, LLC, for the U.S. Department of Energy (DOE) under Contract No. DE-AC36-08GO28308. Funding provided by the U.S. Department of Energy Office of Energy Efficiency and Renewable Energy Wind

Energy Technologies Office. The views expressed in the article do not necessarily represent the views of the DOE or the U.S. Government. The U.S. Government retains and the publisher, by accepting the article for publication, acknowledges that the U.S. Government retains a nonexclusive, paid-up, irrevocable, worldwide license to publish or reproduce the published form of this work, or allow others to do so, for U.S. Government purposes.

References

[1] Sorensen, J. N. and Shen, W. Z. "Numerical modeling of wind turbine wakes." Journal of Fluids Engineering Vol. 124(2) (2002) pp. 393-399.
[2] Yoshizawa, A. and Horiuti, K. "A statistically-derived subgrid-scale kinetic energy model for the large-eddy simulation of turbulent flows." J. Phys. Soc. of Japan. Vol. 54 (1985) pp. 2834-2839.
[3] Martinez-Tossas, L. A. et al. 2016. "A highly resolved large-eddy simulation of a wind turbine using an actuator line model with optimal body force projection."
[4] Churchfield, M. J., et al. 2017. "An Advanced Actuator Line Method for Wind Energy Applications and Beyond. " 35th Wind Energy Symposium, AIAA SciTech Forum, 9 - 13 January 2017, Grapevine, Texas.
[5] Martinez-Tossas, L. A. et al. 2014. "Large eddy simulations of the flow past wind turbines: actuator line and disk modeling."
[6] Luis A. Martínez-Tossas and Charles Meneveau. "Filtered lifting line theory and application to the actuator line model." J. Fluid Mech. (2019), vol. 863, pp. 269292.
[7] Kelley C L and Ennis B L "SWiFT Site Atmospheric Characterization." Sandia National Laboratories Unclassified Unlimited Release (UUR) In: SAND-2016-0216, (2016)
[8] Martinez-Tossas, L. A. et al. 2017. "Optimal smoothing length scale for actuator line models of wind turbine blades based on Gausian body force distribution."
[9] NWTC Information Portal (OpenFAST). URL: https://nwtc.nrel.gov/OpenFAST.
[10] Fleming P, Gebraad P M O, Lee S, Wingerden J-W v, Johnson K, Churchfield M, Michalakes J, Spalart P and Moriarty P "Simulation comparison of wake mitigation control strategies for a two-turbine case" Wind Energy Vol. 18 (2015) pp. 2135-43 (2015)
[11] Atmosphere to Elections (A2e). Maintained by A2e Data Archive and Portal for U.S. Department of Energy, Office of Energy Efficiency and Renewable Energy. https://a2e.energy.gov/projects/wake. January 30, 2019.
[12] Domino, S. P. "Sierra Low Mach Module: Nalu Theory Manual 1.0" Sandia National Laboratories Unclassified Unlimited Release (UUR) In: SAND2015-3107W, (2015), Available: https://github.com/NaluCFD/NaluDoc.
[13] Hsieh, A. S., et al. 2021 "High-Fidelity Wind Farm Simulation Methodology with Experimental Validation." Journal of Wind Engineering & Industrial Aerodynamics. Vol 218 (2021) 104754.
[14] Blaylock, et al. "Comparison of Actuator Line Model and a Filtered Lifting Line Correction Implemented in Nalu-Wind Large Eddy Simulations of the Atmospheric Boundary Layer" Wind Energy Science Conference. May 25-28, 2021
[15] Doubrawa, P., et al. "Benchmarks for Model Validation based on LiDAR Wake Measurements". 2019 J. Phys.: Conf. Ser. 1256 012024